Grain size modulates volcanic ash retention on crop foliage and potential yield loss

Noa Ligot[1,*], Patrick Bogaert[1], Sébastien Biass[2], Guillaume Lobet[3,4], Pierre Delmelle[1]

[1]Environmental Sciences, Earth and Life Institute, UCLouvain, Louvain-la-Neuve, Belgium

[2]Department of Earth Sciences, University of Geneva, Geneva, Switzerland

[3]Agricultural Sciences, Earth and Life Institute, UCLouvain, Louvain-la-Neuve, Belgium

[4]Agrosphere Institute, IBG3, Forschungszentrum Jülich, Jülich, Germany

*corresponding author: Noa Ligot

Email: noa.ligot@uclouvain.be

Tel.: +32 (0)10 473 638

NL ORCID: 0000-0003-1416-3663

Abstract

15 Ashfall from volcanic eruptions endangers crop production and food security, while

jeopardising agricultural livelihoods. As population in the vicinity of volcanoes continues to

grow, strategies to reduce volcanic risks to and impacts on crops are increasingly needed.

18 Current models of crop vulnerability to ash are limited. They also rely solely on ash thickness

(or loading) as the hazard intensity metric and fail to reproduce the complex interplay of other

volcanic and non-volcanic factors that drive impact. Amongst these, ash retention on crop

21 leaves affects photosynthesis and is ultimately responsible for widespread damage to crops. In

this context, we carried out greenhouse experiments to assess how ash grain size, leaf

pubescence and humidity conditions at leaf surfaces influence the retention of ash (defined as

24 the percentage of foliar cover coated with ash) in tomato and chilli pepper plants, two crop

types commonly grown in volcanic regions. For a fixed ash mass load ($\sim$570 g m^{-2}), we found

that ash retention decreases exponentially with increasing grain size and is enhanced when

27 leaves are pubescent (such as in tomato) or their surfaces are wet. Assuming that leaf area

index (*LAI*) diminishes with ash retention in tomato and chilli pepper, we derived a new

expression for predicting potential crop yield loss after an ashfall event. We suggest that the

30 measurement of crop *LAI* in ash-affected areas may serve as an impact metric. Our study

demonstrates that quantitative insights into crop vulnerability can be gained rapidly from

controlled experiments. We advocate this approach to broaden our understanding of ash-plant

33 interaction and to validate the use of remote sensing methods for assessing crop damage and

recovery at various spatial and time scales after an eruption.

Introduction

The livelihood and food security of hundreds of millions of people living near and on volcanoes intricately depend on agriculture (Small and Naumann, 2001; Brown et al., 2015). However, farming activities in these regions are exposed to short-term, i.e. usually less than one year, negative impacts of volcanic eruptions, an issue amplified by the expanding population living under volcanic risk (Brown et al., 2015; Freire et al., 2019). Where cropping activity dominates (for example, in Indonesia), widespread damage to agriculture during eruptive activity arises from crop exposure to ashfall (e.g. Burket et al., 1980; de Guzman, 2005; Tampubolon et al., 2018), causing adverse effects that range from temporary perturbations in leaf physiology to irreversible mechanical damage (Eggler, 1948; Blong, 1984; Grishin et al., 1996; Ayris and Delmelle, 2012). As a result, crop fields impacted by ash deposition produce lower or poor-quality harvests that can translate into significant economic losses to farmers and food shortages at the local or even regional scale, and even more so when subsistence agriculture dominates (Neild et al., 1998; Wilson et al., 2007; Ligot et al., 2022).

In this context, the development of strategies that can support disaster risk reduction and strengthen resilience for agrarian communities in volcanically active regions is critical, especially in less-economically developed countries (FAO, 2021). Such measures require a sound understanding of agriculture vulnerability to ashfall (UNDRO,1980; Jenkins et al., 2015; Craig et al., 2021). Over the past 15 years, a dozen or so of post-eruption impact assessments (post-*EIA*) have contributed to document the responses of farming systems exposed to ash (e.g. Wilson et al., 2007; Wilson et al., 2011; Magill et al., 2013; Blake et al., 2015; Craig et al., 2016a; Craig et al., 2016b; Ligot et al., 2022). These field-based investigations have underpinned the development of empirical relationships that link ash accumulation (also referred to as ash mass load or deposit thickness) to an estimated level of production loss for

different agriculture types characterised by specific vulnerabilities (Wilson and Kaye, 2007; Jenkins et al., 2014; Craig et al., 2021). In parallel, new methodologies harvesting the potential of big Earth observation data acquired from satellite-based sensors (e.g. Landsat, MODIS and Sentinel) and interpretable machine learning are being developed to complement post-*EIA* studies (Biass et al., 2022).

Despite these recent efforts, current ash-loss of crop production relationships remain overshadowed by uncertainties (Jenkins et al., 2015), which are rooted in three main sources. Firstly, they lean on limited observational data, acquired in post-*EIA* studies. Most of these have been conducted in temperate volcanic regions, but tropical and semi-arid environments are increasingly receiving attention. Secondly, it is assumed that ground ash accumulation (thickness or ash mass load) is the principal hazard intensity metric governing impact level on crops. However, other volcanic (e.g. ash grain size, surface composition) and non-volcanic factors (e.g. environmental conditions, plant traits, crop development stage) play a key role in dictating impact and vulnerability (Jenkins et al., 2015; Ligot et al., 2022). Finally, current approaches lack an impact metric that can be applied to assess crop yield loss from ashfall. These limitations are hindering the development of accurate process-based risk assessment models that can inform targeted strategies to build resilience of agriculture-based community in the case of an explosive eruption; for example, in relation to aid allocation, land-use planning and insuring.

Jenkins et al. (2022) estimated that an explosive eruption of *VEI* 4 (Volcanic Explosivity Index, Newhall and Self (1982)) on the island of Java, Indonesia, has on average a 50% probability of affecting ~700 km^2 of crops with 5 kg m^{-2} of ash. The surface area potentially affected by ash fallout is ~17 times larger for an eruption of *VEI* 5. Ash deposits thin exponentially from the source. Close to the vent, ash fallout usually results in destructive impacts, e.g. smothering of

84 the vegetation and direct mechanical breakage of plant's parts (leaves, twigs, stem) (Ayris and

Delmelle, 2012; Arnalds, 2013; Jenkins et al., 2015; Craig et al., 2021). With increasing

distance from the vent, impacts gradually become less severe disturbances. Thin ash deposits,

87 able to affect several hundred to thousands of square kilometres, retain the potential to cause

serious crop yield loss without threatening plant structural integrity (Magill et al., 2013; Ligot

et al., 2022). At distal sites, in the absence of structural damage to plants, the capacity of ashfall

90 to initiate damage to crop yield hinges on the capacity of leaves coated with a thin ash deposit

to operate photosynthesis and produce biomass. While the release of harmful chemical

compounds from ash can cause leaf tissue injuries and affect photosynthesis, this effect, if

93 occurring, is limited to ash emissions from phreatic and phreatomagmatic eruptions (Le Guern

et al., 1980; Ayris and Delmelle, 2012). For purely magmatic explosive events, impact on crops

over a wide area far from the volcano primarily relates to the shading effect exerted by the

96 presence of solid particles on leaf surfaces, reducing light interception and decreasing

photosynthetic activity (Thompson et al., 1984; Hirano et al., 1995). Thus, ash retention on

foliage (i.e. the percentage of the leaf surface area covered with ash) is a critical variable for

99 developing accurate models that can assess and predict widespread impacts on crop production

from ashfall. Although ash grain size, leaf pubescence and ambient humidity have been

suspected to affect ash retention on foliage, we are still lacking a (i) systematic investigation of

102 factors controlling ash retention on foliage and (ii) quantitative impact metric reflecting crop

production loss.

Here, we adopt an experimental setup to investigate the influence of ash grain size, leaf

105 pubescence and humidity conditions at leaf surfaces on ash retention by crop foliage using

tomato and chilli pepper as model plants. By integrating the effect of both volcanic and non-

volcanic factors on ash retention, we formulate a novel conceptual model that uses *LAI* as the

108 impact metric for predicting crop yield loss when ash deposited on plants does not threaten

their integrity.

Material and methods

111 *Plant material and growing conditions*

Tomato (*Solanum lycopersicum* L.) and chilli pepper (*Capsicum annuum* L.) were chosen to

illustrate contrasting behaviours between plants of agronomical interest; they have a similar

114 stand in early growth period, but tomato has hairy leaves whereas chilli pepper has glabrous

leaves. The experiment took place in Belgium. The seeds were sown in a sieved peat-based

compost (pH 5-6.5) maintained at 24 °C. Four weeks after sowing, the seedlings were

117 transplanted in 1-litre plastic pots also filled with peat-based compost. The average day and

night temperatures in the greenhouse were 30 and 24 °C, respectively. Due to summer heats

in Belgium, temperature during the day occasionally rose above 35 °C. Combined with

120 natural light, the use of *LED* lamps (120 µmoles $m^{-2}\,s^{-1}$) provided a 16 h-photoperiod. Tomato

and chilli pepper plants were watered three times a week. They were exposed to ash six weeks

after sowing, when tomato and chilli pepper were at the seven- and eight-leaf stage,

123 respectively. The corresponding plant heights were ~40 and ~30 cm. The foliage surface area

was ~400 and ~100 cm² for tomato and chilli pepper, respectively.

Simulated ash deposition

126 We investigated the influence of ash grain size on the ability of tomato and chilli pepper

leaves to retain ash under dry and moist conditions. Six ash size ranges were tested, namely ≤

90, 90-125, 125-250, 250-500, 500-1000 and 1000-2000 µm. Each size range was tested in

129 combination with either dry or wet leaf surface conditions, i.e. a total of 24 treatments for

both crops. A treatment consisted of 15 replicates, corresponding to 360 measurements in

total. The ash material was obtained by crushing a phonolite rock (bulk composition: SiO_2 =

52.5, Al_2O_3 = 21.8, K_2O = 9.6, Na_2O = 7.8, Fe_2O_3 = 2.9, CaO = 1.5, TiO_2 = 0.3, MgO = 0.2

wt.%; density = 2.54 g cm^{-3}; Van Den Bogaard and Schmincke, 1984) obtained from a quarry

close to Laacher See volcano in Germany. The shape characteristics of the six ash size

fractions obtained by grinding the Laacher See phonolite were examined by scanning electron

microscopy (*SEM*). The *SEM* images (Fig. S1) reveal that, regardless of their size, most

particles are blocky, but rounded and platy shapes also occur. Similar shapes are commonly

reported for ash particles from explosive eruptions (e.g. Wohletz (1983); Coltelli et al. (2008);

Nurfiani and Bouvet de Maisonneuve (2017)). However, the vesicular ash type that is also

often associated with the magma fragmentation of gas-rich magmas cannot be generated by

rock grinding and was absent in our experimental ash material. The crushed phonolite was dry

sieved for 10 minutes using an AS 200 Control Retsh vibrating sieve shaker with six sieves

(90, 125, 250, 500, 1000, 2000 µm). The five size fractions coarser than 90 µm were wet

sieved to remove particles < 90 µm. The grain size distribution of the six ash size ranges was

measured between 0.04 and 2000 µm by laser diffraction (Beckman Coulter LS13 320) (Fig.

S2). The median diameter was equal to 5, 98, 174, 401, 774 and 1465 µm for the ≤ 90, 90-

125, 125-250, 250-500, 500-1000 and 1000-2000 µm ash size ranges, respectively.

An ash load of ~570 g m^{-2} was selected for the experiments. Assuming a bulk density of 1 g

cm^{-3} for the ash deposit (Eychenne et al., 2012), this corresponds to a relatively thin deposit of

~0.6 mm (i.e. considering a bulk deposit density of 1 g cm^{-3}, Eychenne et al. (2012)), best

representing accumulations encountered at distal sites (and over wide areas) affected by ash

fallout from explosive eruptions (Fierstein and Nathenson, 1992; Jenkins et al., 2022). Pre-

tests carried out with higher ash loads (≥ 1000 g m^{-2}) already led to lodging of some tomato

and chilli pepper plant specimens, a phenomenon that needed to be avoided in order to

maximise the experiment's reproducibility. Neild et al. (1998) and Craig (2015) consider that

156   an ash mass load of 6-30 kg m^{-2} on plants leads to mechanical damage. Our observations

indicate that lower loads can affect crop plants. In other words, the threshold value above

which mechanical injury occurs varies with plant phenology (i.e. the combination of genotype

159   and environment).

The selected ash load was applied uniformly to each plant using a homemade ashfall

simulator (Fig. S3). The device consists of a 135 cm-high *PVC* tube (of diameter 29.5 cm)

162   with three 1-mm opening meshes placed at 75, 110 and 120 cm from the tube base. The ash

fractions <1000 µm were poured carefully through a 2 cm-mesh sieve installed on the top of

the *PVC* tube. Bouncing of the ash particles passing through the three inner 1-cm sieves

165   allowed formation of a uniform deposit. Application of the coarsest ash (1000-2000 µm) was

carried out with the same device, but the inner meshes were removed. Wet conditions at leaf

surfaces were obtained by spreading ~1.5 g of water on each plant using a commercial manual

168   sprayer held one meter above the ground. In order to simulate the presence of water droplets

on plant leaves, we applied four sprays of water, one in each cardinal direction just before ash

treatment. Water spraying of the plant foliage, ash application and photo acquisition all took

171   place within the black chamber. Less than five minutes elapsed between the spraying

operation and photo acquisition of the ash-treated plant (Fig. S4).

Estimating the foliar cover from digital photos

174   We took photos of each plant before and immediately after ash treatment (Fig. S4). To

minimise uncontrolled variations in light colour and brightness, plants were photographed in a

1.6 x 1.2 x 2.2 m black chamber equipped with four led bulbs (6.5 W, cold white, Fig. S3 and

177   S4). We used a DX Nikon camera with an AF-S DX NIKKOR 18-55mm f/3.5-5.6G VR II

lens mounted on a 0.9 m-high tripod. Sheets of paper were placed on the floor and plant pot to

produce a uniform background. A ribbon placed in a fixed position provided a reference scale.

180 We analysed the digital photos taken just before and after ash application with ImageJ 1.52 (Schindelin et al., 2015). The foliar cover, a measure of the vertical projection of exposed leaf area, was estimated using a dedicated macro (https://github.com/NoaLigot/ImageJ-macro.git).

183 While digital photos are recorded as a raster of red/green/blue (*RGB*) pixels, the values are not standardised and can vary depending on the camera (Darge et al., 2019). The ImageJ macro transforms the *RGB* colour space into the International Commission on Illumination (*CIE*)

186 1976 L*a*b* colour space (McLaren, 1976), which has linear measures of lightness (L*) and two colour dimensions (a* and b*). The a* dimension represents a spectrum from green (negative) to magenta (positive) and the b* dimension represents a spectrum from blue

189 (negative) to yellow (positive). The a* attribute is useful to identify green pixels and was used in the ImageJ macro to identify and select green parts of leaves. Values of 1 and 0 are attributed to a green and non-green (background) pixel, respectively. This allows delineation

192 of the shape of the green leaf portion and calculation of its surface area.

Data treatment

The percentage of foliar cover coated with ash was inferred for each plant by comparing the

195 foliar cover estimated from the image analysis, before and after ash application. A Tukey *HSD* (Honest Significant Difference) test was applied to determine if means differ between treatments. Tomato and chilli pepper plant measurements carried out under dry and wet leaf

198 surface conditions were processed separately, i.e. four sub-datasets were used in order to compare the means separately for each combination of crops and moisture conditions.

Results

201 *Foliar cover coated with ash*

The percentage of foliar cover coated with ash ranged from 0 to 99%, with an average value of 36 ± 33% (Table S1). The effect of ash grain size, humidity conditions at leaf surfaces and leaf pubescence on the foliar cover coated with ash is illustrated in Fig. 1. In general, foliar cover coated with ash increased with decreasing ash grain size. Grain size ≥ 500 µm covered only 10% of the foliar cover, with coverage increasing up to ~90% for ash ≤ 90 µm. Wetting of tomato and chilli pepper leaves prior to ash application had no significant effect on the retention of fine ash (≤ 90 µm). Nevertheless, significant higher tomato and chilli pepper leaf surface coverages (+17 ± 5% and +31 ± 10%) were inferred for intermediate ash grain sizes between 90 and 500 µm (Table S1, S2). We also note that for the ash grain size ranges 125-250 and 250-500 µm in dry conditions, coverage of tomato leaves with ash was significantly greater, by ~30 and 20% on average, compared to chilli pepper leaves.
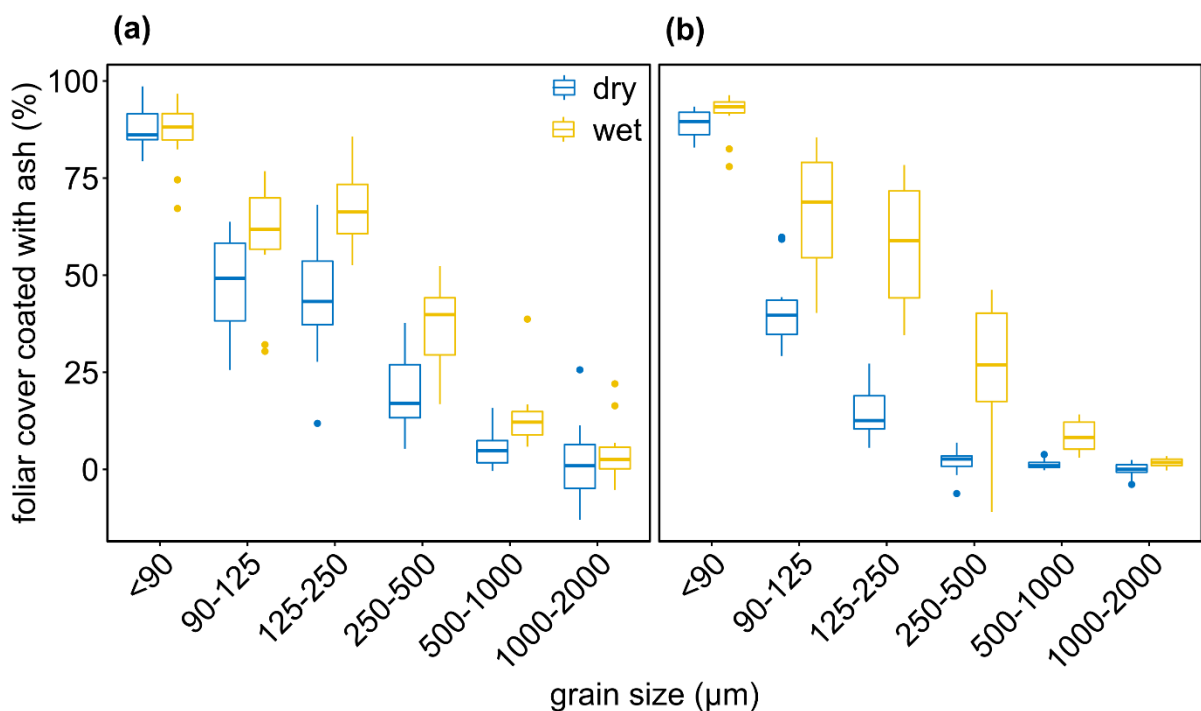
Figure 1: Percentage of foliar cover coated with ash for tomato plant, i.e. which has pubescent leaves, (a) and chilli pepper plant, which has glabrous leaves (b). The percentage of foliage cover was measured for the six grain size ranges tested in dry and wet conditions at leaf surfaces. Each boxplot represents 15 repetitions. The median value sits within the box and represents the centre of the data. Fifty % of the data values lie above the median and 50% lie below the median. Measurement outliers are displayed as dots.

Quantifying ash retention as a function of grain size

Using the experimental results obtained for tomato and chilli pepper (Fig. 1), we predicted the

222   percentage of foliar cover coated with ash as a function of grain size, when leaf surfaces are

dry or wet. Five convex models (i.e. exponential decay, power curve, rectangular hyperbola,

asymptotic curve and logarithmic curve) were fitted to the data points using the *aomisc* and

225   *nlme* packages in *R* (Onofri, 2020; Pinheiro and Bates, 2022) (Fig. S5). The median grain size

was used to represent the corresponding grain size range. A lack-of-fit sum of squares test

was applied to evaluate the relevance of each model. Since the five models have different

228   numbers of parameters, their test statistics (F*) could not be compared directly. Instead, the

models were assessed based on their *p*-values (Table S3). All the models have *p*-values > 5%,

with no evident lack-of-fit. The exponential decay model had the highest *p*-value for the four

231   sub-datasets (0.82, 0.98, 1, 1 for dry tomato, wet tomato, dry chilli pepper and wet chilli

pepper, respectively) and it was chosen for the predictions.

Quantile regressions using the exponential decay model indicate that for 500 µm ash particles,

234   there is a 50% chance to cover ~10 and ~27% of tomato foliar cover in dry and wet

conditions, respectively (Fig. 2). Similarly, for chilli pepper, foliar covers of <1 and 20% are

estimated in dry and wet conditions, respectively. By the same tenet, there is a 50%

237   probability that ash with a median of 63 µm in diameter covers up to ~67% (dry conditions)

and ~77% (wet conditions) of the foliar cover in tomato, and ~51% (dry conditions) and

~78% (wet conditions) of the foliar cover in chilli pepper.

240
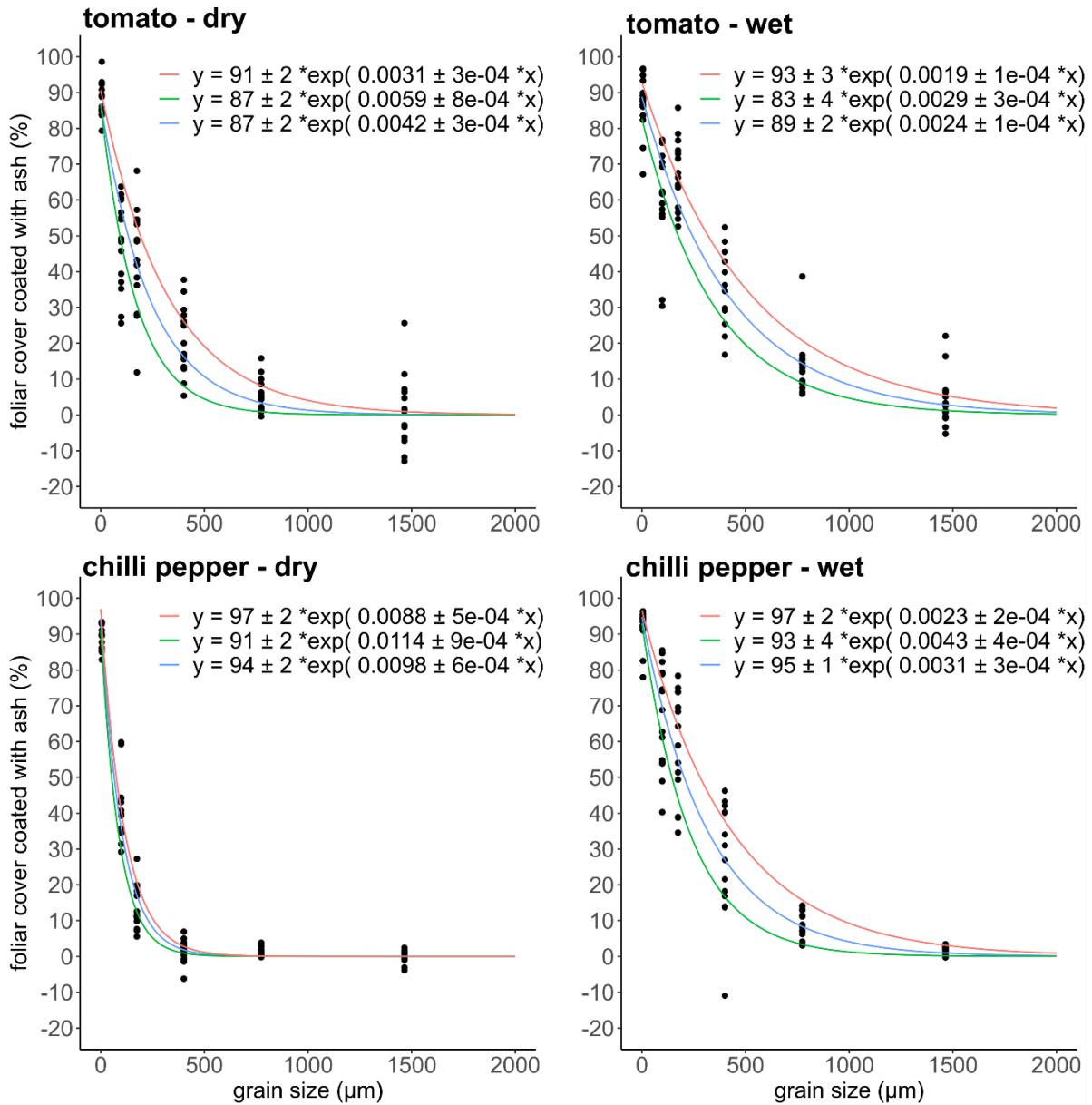
Figure 2: Quantile regression with the first quartile (green), median (blue) and third quartile (red) for tomato and chilli pepper plants in dry and wet conditions at leaf surfaces.

Distribution of ash retention on the foliar cover

In addition to controlling ash retention on leaves, grain size, conditions of humidity at leaf surfaces and leaf pubescence affect the location of ash retention (Fig. 3). For tomato plants in dry conditions, ash ≤ 90 µm tended to be lodged on the leaf surface wherever it had settled. For glabrous chilli pepper leaves, leaf angle dictates if the ash particles remain on the leaf surface after deposition or slide off and relocate elsewhere. Ash with intermediate grain sizes between 90 and 500 µm behaved differently, depending on humidity conditions. For both

tomato and chilli pepper plants, the ash material was found mainly along the primary and

secondary veins of the horizontal upper leaves when they were dry. However, in wet

conditions, ash was more homogeneously distributed over the leaf surface. Coarser ash (≥ 500

µm) accumulated preferentially in the folds of growing leaves.

		≤ 90 µm	90-125 µm	125-250 µm	250-500 µm	500-1000 µm	1000-2000 µm	control
tomato	dry							
	wet							
chilli pepper	dry							
	wet							

Figure 3: Photos processed with ImageJ of tomato and chilli pepper plants before (control) and after exposure to ~570 g m^{-2} of ash varying in grain size ($\leq$ 90, 90-125, 125-250, 250-500, 500-1000, 1000-2000 µm) and in dry and wet conditions at leaf surfaces. The part of the foliar cover depicted in black corresponds to the green leaf surface area that was not covered with ash. The image surface area is equivalent to ~800 cm². The original photos of the ash-covered plants are provided as supplementary material (Fig. S6).

Discussion

Influence of grain size on ash retention

The foliar cover coated with ash increases exponentially (from ~10 to 90%) when grain size

decreases from 500 to 90 µm, whether in dry or humid leaf conditions (Fig. 2). This

relationship was established for a single ash mass load (~570 g m^{-2}). For ash in the

intermediate size range, a higher load could result in enhanced retention of the particles,

particularly along the primary and secondary leaf veins as these consist of less elastic tissues

270   that can better absorb the kinetic energy of impinging ash particles of intermediate grain size.

However, for fine ash, we do not expect more retention to occur if tomato and chilli pepper

leaves were exposed to higher loads because a large proportion of the uncovered foliage is

273   comprised of leaves that, due to their steep angle, cannot retain ash particles efficiently. As

mentioned earlier, coarse ash particles tend to lodge primarily on leaf folds. Thus, their

retention on foliage will likely be limited by the number of leaf folds. Overall, we anticipate

276   that for ash load values >570 g m^{-2}, the exponential dependence of ash retention on ash grain

size will start to degrade and instead, a linear relationship would be a better model. The

increased ash retention when grain size decreases is in accordance with the field observations

279   of Miller (1967) after the 1963 eruption of Irazú volcano, Costa Rica, who found a higher

degree of retention of the smaller particles by crop foliage (alfalfa, maize, bean, beet,

cabbage, carrot, pea, pepper, potato, radish and squash). Johnson and Lovaas (1969) and

282   Witherspoon and Taylor (1970) reached a similar conclusion after dusting various crops

(alfalfa, maize, squash, soybean, sorghum, peanut and clover) with quartz powders differing

in grain size (88-175 and 175-350, and 44-88 and 88-175 µm, respectively).

285   The fate of a solid particle falling from the atmosphere and hitting a leaf surface will depend

on how much of its initial kinetic energy is absorbed through tissue deformation (Vogel,

1989; Niklas, 1999; Benson, 2015). Ignoring aggregation processes and considering a

288   constant particle bulk density, the coarser the particles, the larger their terminal fall velocity

and thus, kinetic energy (Dellino et al., 2005; Benson, 2015), simply reflecting that mass

increases with grain size. If particles retain enough kinetic energy after impact, they can

291   bounce back and be ejected off the leaf or deposited elsewhere (Gregory, 1961; Chamberlain,

1967; Starr, 1967; Chamberlain and Chadwick, 1972). Otherwise, they will settle on the upper

side of leaves, although they may be subsequently displaced as new particles impinge the leaf

294   surface. Based on the drag model for non-spherical particles of Bagheri and Bonadonna

(2016), we estimated the terminal fall velocity of individual particles of 10, 100, 170, 410,

710 and 1470 µm, representing the median values of the six ash size ranges used in our

297   experiment. Terminal fall velocity increases with grain size and is five times lower for

particles of 100 µm diameter (assimilated to the fine ash fraction) than for particles of 410 µm

diameter (corresponding to coarse ash) (Table S4). This result suggests that the kinetic energy

300   of the finest ash particles is ~10,000 times smaller than that of the coarsest material. The low

kinetic energy of fine particles probably explains why ash in the ≤ 90 µm size fraction

produces a greater foliar cover compared to ash ≥ 500 µm (Fig. 2). In contrast, coarse ash

303   particles with higher kinetic energy will tend to lodge on less elastic leaf structures, such as

primary and secondary veins and folds (Fig. 3). As mentioned above (section Material and

methods), an inherent limitation of our experimental study is that the ash material did not

306   contain the vesicular particles that are usually found in various proportions in ash fallout from

explosive eruptions. We speculate that the irregular shape of vesicular ash could enhance

retention on foliage, perhaps even more so if the leaf surfaces are pubescent or wet. Thus, our

309   measurements may be regarded as conservative estimates.

Influence of leaf pubescence on ash retention

On average, ash particles in the intermediate size range 125-500 µm cover ~25% more foliar

312   cover in tomato than in chilli pepper (Fig. 2, Table S1). This is attributed primarily to the

presence of leaf hairs in tomato. Sæbø et al. (2012) and Ram et al. (2012) demonstrated that

dust accumulation on the foliage of various trees and shrubs is proportional to leaf hair

315   density. Leaf hairs enhance dust collection area and capacity to absorb the falling particles'

kinetic energy. In addition, leaf pubescence may prevent particles from sliding off the leaf

surface. By increasing friction on particles, leaf hairs counteract the gravity force generated

318   by mass loading on the leaf surface which pulls a leaf downward (Smith and Staskawicz,

1977). In our experiments, ash $\leq$ 90 µm adhered to the tip of pubescent leaves with a steep

inclination angle in tomato plants, whereas it barely encroached on the glabrous surface of

321   chilli pepper leaves (Fig. 3). Previous field observations of ash-impacted crops also highlight

a stronger adherence of ash on pubescent leaves (such as barley, corn, tobacco, tomato and

apple tree) and hairy fruits (such as peach, apricot, kiwi-fruit, strawberry and raspberry)

324   (Miller, 1967; Cook et al., 1981; Wilson et al., 2007; Sword-Daniels et al., 2011; Ligot et al.,

2022). Witherspoon and Taylor (1970) concluded that the pubescent leaves of squash and

soybean favour a uniform retention of quartz particles (88-175 µm). In contrast, the glabrous

327   leaves of rose plants exposed to the 1963 eruption of Irazú volcano, Costa Rica, collected

little ash material (Miller, 1967).

Influence of humidity conditions at leaf surfaces on ash retention

330   Wetting of leaves prior to application of ash with an intermediate grain size of 90-500 µm

increased the foliar cover coated with ash of tomato and chilli pepper by 17 $\pm$ 5% and 31 $\pm$

10%, respectively (Fig. 2, Table S2). We also noted that the ash deposit that formed on pre-

333   wetted leaves appeared more homogeneous compared to that observed when the leaf surface

was dry (Fig. 3). Similarly, Miller (1967) reported during the 1963 eruption of Irazú that wet

leaf surfaces facilitated retention of ash < 300 µm and formation of a homogeneous deposit.

336   Enhanced ash retention on wet leaves likely relates to the surface tension generated by water

molecules present on the leaf surface (Tabor, 1977; Israelachvili, 2011). Conversely, as plant

leaves are hydrophobic (Bhushan and Jung, 2006), more water on leaves, such as after a

339   heavy or prolonged light rain, could lead to formation of large water droplets able to erode

particle from the leaf surface, thereby reducing ash retention.

Modelling potential yield loss in tomato and chilli pepper plants exposed to ash

342   Our experimental results indicate that ~570 g m^{-2} fine ash can readily cover the upper side of

      leaves (Fig. 2). Assuming an ash material comprised of spherical particles 90 µm of diameter

      and with a density of 2.54 g cm^{-3} (i.e. the density of phonolite), we calculated that a mass load

345   as low as ~8.6 g m^{-2} can form a monolayer deposit on a leaf surface. While this estimate

      represents an oversimplified situation, it is more than fifty times less the ash load (~570 g m^{-2})

      used in our experiment. Since fine particles are ubiquitous– albeit in various proportions – in

348   ash fallout (Rust and Cashman, 2011; Costa et al., 2016), an ash coating on leaf surfaces is

      likely to be the rule in vegetated areas affected by explosive eruptions. Importantly, the

      presence of solid particles on foliage exerts a shading effect, which reduces light interception

351   (*LI*, dimensionless) by leaves (Thompson et al., 1984; Hirano et al., 1990). For example,

      Hirano et al. (1991) measured a ~20% decrease in *LI* after treating mandarin tree leaves with

      only 4 g m^{-2} of road dust (0.1-100 µm). Similarly, deposition of 10 g m^{-2} of ash (0-100 µm)

354   on cucumber plants led to a ~20% reduction in *LI* (Hirano et al., 1992).

      Considering that *LI* drives net photosynthesis rate and thereby, total biomass production

      (Wilson, 1967; Biscoe et al., 1977; Monteith, 1977; Weraduwage et al., 2015), we contend

357   that even a thin ash deposit on crop leaves can drive yield loss. Thus, the interference of ash

      with *LI* provides an indirect mean to predict the potential crop production loss for ash mass

      loads below the threshold (~6-30 kg m^{-2} mass load) of direct mechanical damage to plants.

360   Although we did not measure *LI* in our experiment, this parameter can be inferred using the

      following expression (Monteith, 1969):

$$LI = (1 - e^{-k \times LAI}) \tag{1}$$

363   where *k* is the light interception coefficient (dimensionless). The temporal evolution of *LAI*

      during plant growth has been documented for tomato and chilli pepper in several studies (e.g.

Campillo et al., 2010; Monte et al., 2013; Al Mamun Hossain et al., 2017; Mendoza Perez et

al., 2017), allowing the estimate of *LI via* Eq.(1).

In light-limited situation, i.e. the other growth parameters (e.g. water and nutrient status)

being optimum, the daily biomass accumulation by crop canopy ($CBIO_c$, g m^{-2} day^{-1}) depends

on *LI* according to (Monteith, 1972; Hatfield, 2014):

$$CBIO_c = Q \times LI \times RUE \tag{2}$$

where Q is the incident radiation (MJ m^{-2} day^{-1}) and RUE (g MJ^{-1}) the radiation use

efficiency. Representative values for Q in Belgium (10.6 MJ m^{-2} day^{-1}, warm temperate

humid climate, Solargis, 2022) and RUE are available from the scientific literature (Table S5).

The crop harvested biomass ($CBIO_h$, g m^{-2} day^{-1}) is calculated as the sum of the $CBIO_c$ in the

time period considered (i.e. number of days elapsed between transplanting and harvest)

multiplied with the harvest index, i.e. the fraction of the total aboveground biomass allocated

to the harvested parts of the plant (*HI*, dimensionless) (Kemanian et al., 2007; Hay, 2008):

$$CBIO_h = \sum_{sowing}^{harvest} CBIO_c \times HI \tag{3}$$

Figure 4 depicts the concepts underpinning Eqs. (1), (2) and (3).

We consider two effects of ash on plant yield: reduction in *LAI* and premature biomass

senescence. The former leads to lower accumulated biomass after formation of the ash

deposit, whereas the latter is responsible for a loss of biomass that accumulated prior to ash

fall. We hypothesise that *LAI* reduction and biomass dying in crop plants exposed to ash is

directly proportional to the percentage of foliar cover coated with ash deposits (Fig. 2),

presupposing that ash-affected leaves lose their ability to perform photosynthesis efficiently.

Based on this, and using Eqs. (1), (2) and (3), potential crop yield loss ($CYL_\%$, %) can be

387 deduced by comparing the harvested biomass in the absence ($CBIO_h^{no\ ash}$) and presence

($CBIO_h^{ash}$) of ash (see Supplementary materials):

$$CYL_\% = 100 \times \frac{CBIO_h^{no\ ash} - CBIO_h^{ash}}{CBIO_h^{no\ ash}} \qquad (4)$$
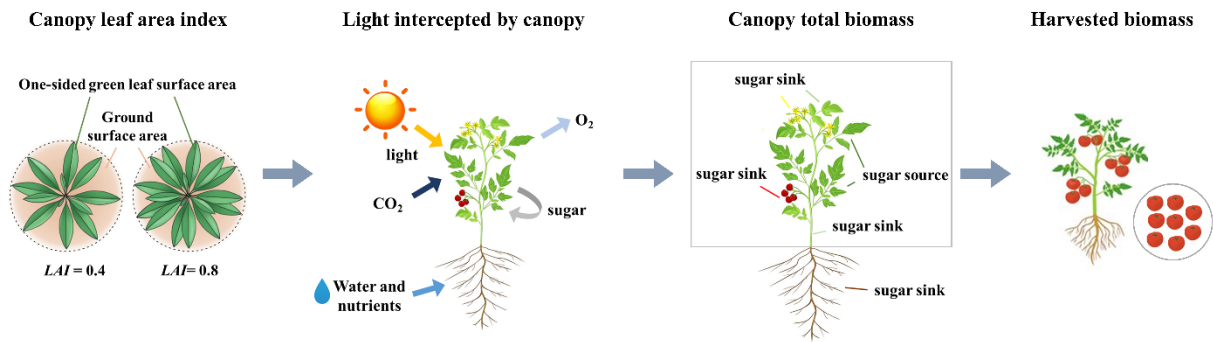
390

Figure 4: Cartoon conceptualising the relationships between canopy leaf area index (*LAI*), light interception by canopy, canopy total biomass and harvested biomass.

393 To illustrate our approach, we estimated $CYL_\%$ for tomato and chilli pepper plants exposed to

~0.6 mm (~570 g m^{-2}) of ash. We tested different ash size distributions and evaluated the

influence of humidity conditions at leaf surfaces on ash retention. Two scenarios of plant

396 exposure to ashfall were considered: one in which 25% of the plant growth period is

completed (i.e. 32 days after transplanting for tomato and 57 days after transplanting for chilli

pepper), and one in which 75% is achieved (i.e. 97 days after transplanting for tomato and

399 172 days after transplanting for chilli pepper). The daily *LAI* evolution of tomato and chilli

pepper plants during growth was computed in *R* using published data (Fig. S6).

In our model, the entire plant canopy received the same amount of ash, although some leaves

402 may be less exposed due to their position on the stem. As the ash mass load is low (570 g m^{-2}), we also considered that ash deposition on leaves neither halt plant growth nor production

of new leaves (Neild et al., 1998; Ligot, 2022). On the day of the eruption, the *LAI* is reduced

405 by an amount corresponding to the percentage of foliar cover coated with ash. On the

following days, it re-increases as new leaves formation resumes at a rate similar to that before

exposure to ash. If time permits, the *LAI* may reach a value identical to that of a plant that

408   would not have received ash. The calculated temporal evolution of the *LAI* of tomato plant

that has completed 25% of its growth period when it receives ash (90-125 µm in diameter,

mass load of ~570 g m^{-2}) in dry conditions is illustrated in Fig. 5a. A similar temporal

411   evolution of *LAI* is obtained for chilli pepper (Fig. S7).

The presence of ash on plant canopy may lead to premature leaf senescence (as reported by

Miller, 1967; Neild et al., 1998; Wilson et al., 2007; Ligot et al., 2022), impacting *CBIO$_h$* (Eq.

414   3). To account for this effect, we subtracted the ash-coated leaf biomass from the total canopy

biomass, the latter being comprised of the leaves and stem. For tomato and chilli pepper

plants, leaf biomass represents ~60% of canopy biomass (Kleinhenz et al., 2006; Elia and

417   Conversa, 2012; Poorter et al., 2015). The leaf biomass fraction affected by ash can be

inferred from Fig. 1. Resolving Eqs. (1) and (2), the temporal evolution of *CBIO$_c$* for tomato

or chilli pepper subjected to ash can be predicted. Fig. 5b illustrates this for tomato plant

420   exposed in dry conditions to ash deposition (90-125 µm in diameter; mass load of ~570 g m^{-2})

32 days after transplanting (i.e. at 25% of growth period). Since the leaf-to-canopy biomass

ratio and percentage of leaf biomass covered with ash which dies are equal for both crops

423   (Table S5, Kleinhenz et al., 2006; Elia and Conversa, 2012; Poorter et al., 2015), a similar

trend is inferred for chilli pepper (Fig. 6).
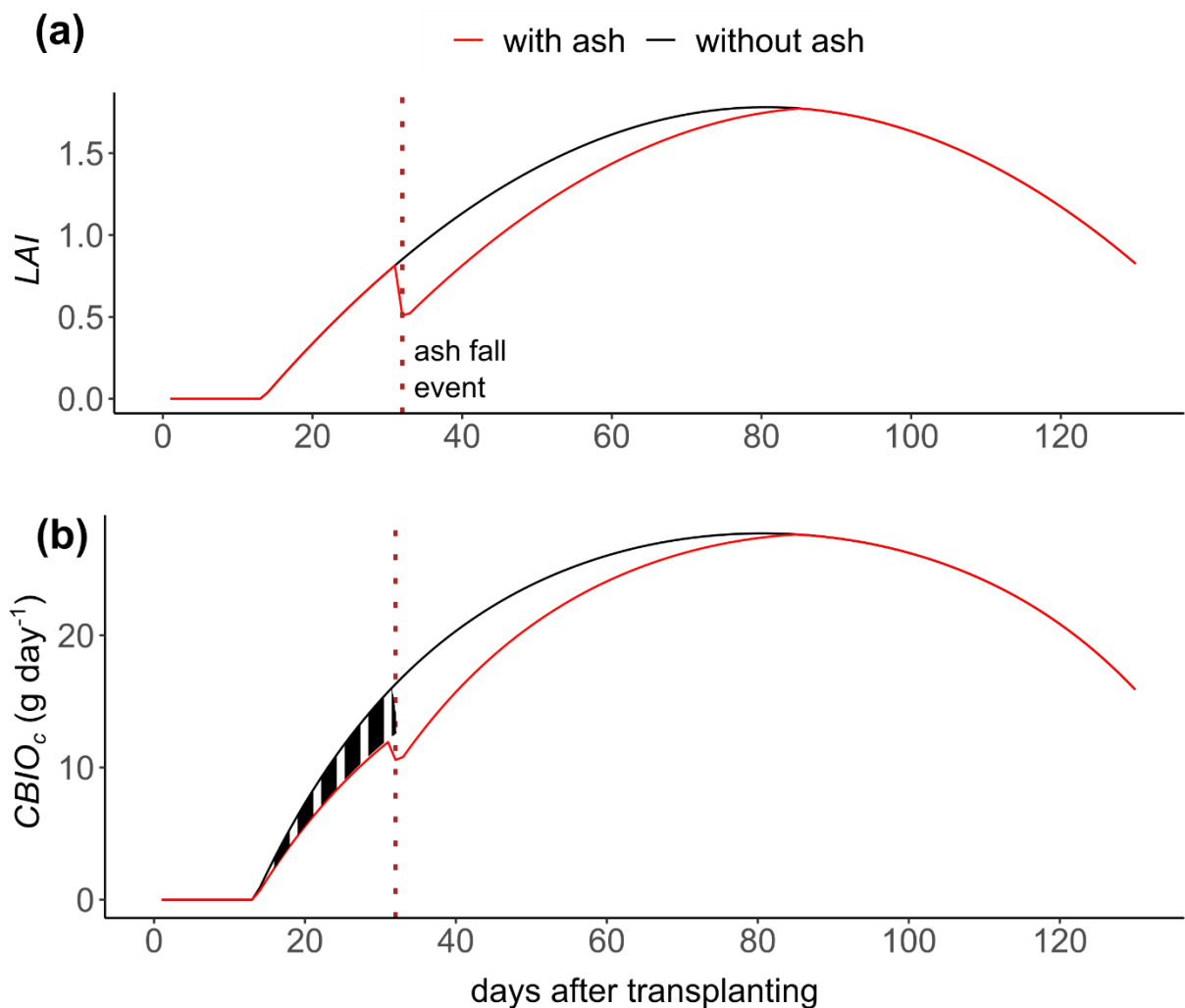
Figure 5: Temporal evolution of leaf area index (*LAI*) (a) and daily biomass accumulation (*CBIO_c*) (b) of tomato plant exposed to ~570 g m^{-2} of ash (size range: 90-125 µm) 32 days after transplanting (i.e. at 25% of the growth period) in dry leaf surface conditions. The hatched area represents the leaf biomass produced by the plant before the ashfall event and which will undergo premature senescence after it. The ash covered leaf biomass is inferred from the leaf-to-canopy biomass ratio (i.e. 60%) and the percentage of leaf biomass covered with ash (i.e. 48% for tomato in dry leaf surface conditions, Table S1).

As detailed above, ash impact on *CBIO_h* is modulated by different factors, including the *LAI* fraction that becomes photosynthetically inactive due to the presence of ash coatings on leaves (i), number of days elapsed between ash deposition and emergence of new leaves (ii), leaf-to-canopy biomass ratio (iii), and percentage of leaf biomass covered with ash and which eventually dies (iv). Our model calculations revealed that crop growth period determines the relative importance of each of these factors in determining *CYL_%*. For example, if 90 µm ash affects tomato and chilli pepper plants in dry conditions at 25% of their growth period, *CYL_%*

is most sensitive to (i) and (ii), whereas for older plants that have completed 75% of their

441   growth, (iii) and (iv) are the main factors driving $CYL_\%$ (see Supplementary materials).

In order to assess the error on $CYL_\%$ estimates, we applied a stochastic approach with 10,000

simulation runs using a random value for each of the four factors (as listed above) that can

444   influence the final model output. We posited that the values taken by factors (iii) and (iv)

follow a gaussian distribution (Table S5), whereas variable (i) and (ii), which are always in

the range 0-1 and positive, respectively, are described by a truncated gaussian distribution.

447   Fig. 6 shows the uncertainties on $CYL_\%$ as computed by fitting the first and third quartiles

around the median $CYL_\%$ value for tomato and chilli pepper plants exposed to ash of different

grain sizes, either in dry or wet leaf conditions. Calculations were repeated for plants that

450   receive ash when at 25 and 75% of their growth period. For tomato, $CYL_\%$ increases with

decreasing ash grain size (Fig. 6). Tomato plants at 25% of their growth may experience a 2-

17% decrease in yield depending on grain size and humidity conditions at leaf surfaces. A

453   significantly higher $CYL_\%$ (0-42%) is anticipated when ash affects plants at 75% of their

growth. A similar pattern emerges for chilli pepper where $CYL_\%$ varies between 1-17 and 0-

46% when considering that the plant receives ash when at 25 and 75% of its growth period,

456   respectively (Fig. 6). For intermediate ash grain sizes between 125 and 500 µm, the $CYL_\%$ is

5, 3, 8 and 4% greater for tomato compared to chilli pepper when exposure to ash occurs at

25% of the growth in dry conditions, 25% of the growth in wet conditions, 75% of the growth

459   in dry conditions and 75% of the growth in wet conditions, respectively.
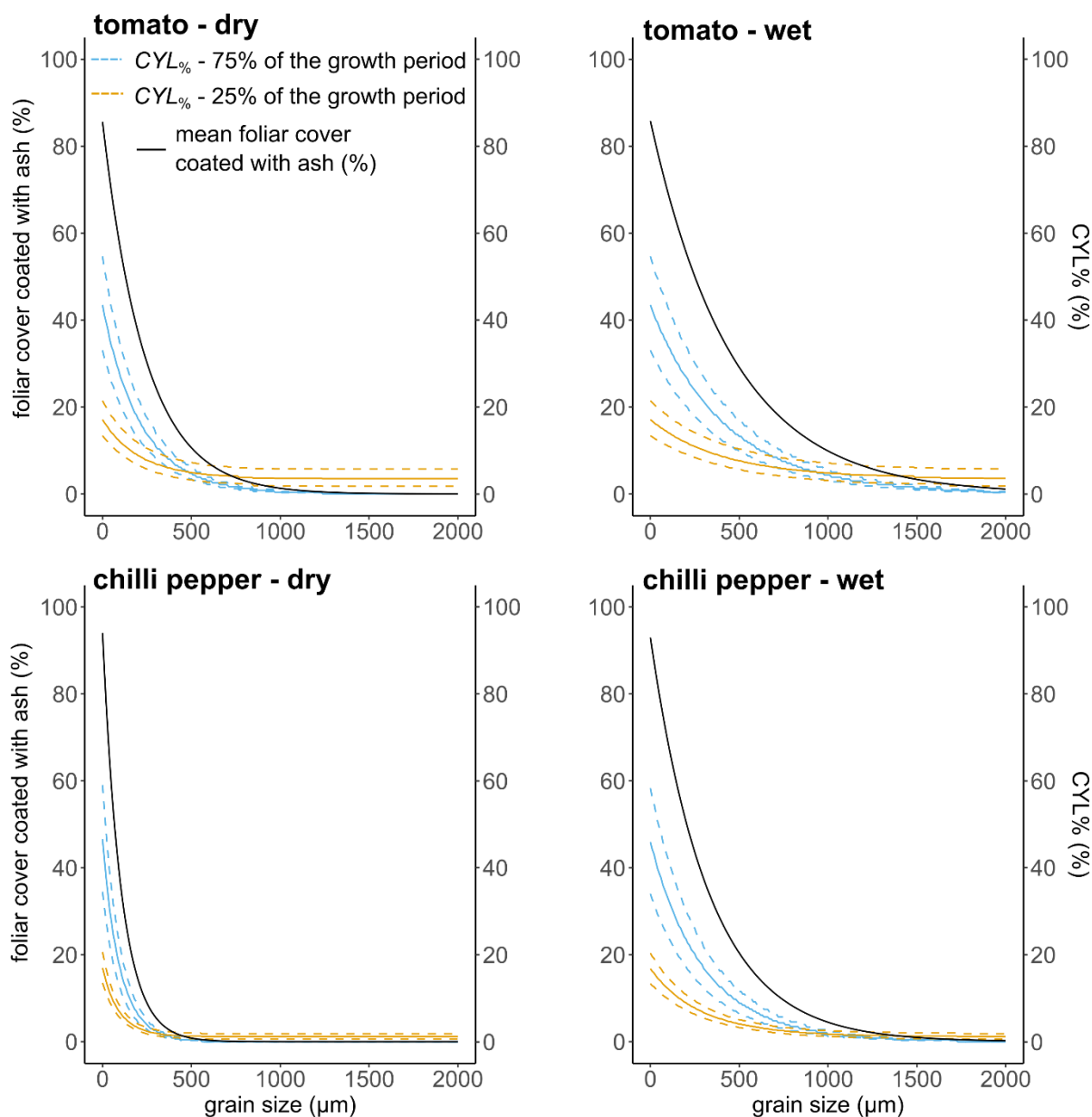
Figure 6: Potential crop yield loss ($CYL_\%$, first quartile, median and third quartile) estimated for tomato and chilli pepper plants as a function of ash grain size in dry and wet conditions at leaf surfaces.

Towards using LAI as an impact metric for predicting potential yield loss in ash-affected

crops

While deployment of field-based post-*EIA* will continue to enrich our understanding of ash-

loss of production relationships, progress is contingent on eruption occurrence, site

accessibility, limited field time, variations in environmental conditions and incomplete ranges

of ash characteristics such as thickness and grain size (Jenkins et al., 2015). Here, we have

471 shown, using established theories of plant-physiological processes (Monteith, 1969; Monteith, 1972), how empirical data from experimental testing can be transformed into quantitative insights for predicting potential yield loss in tomato and chilli pepper crops exposed to ash.

474 Changes in *LAI* and premature biomass loss in ash-affected crops are interpreted as dependent on ash retention on leaves, a process influenced by grain size, plant traits and environmental conditions (Fig. 1). Here, we exclude the possible effect of ash surface composition on ash

477 retention. As detailed in Eqs. (1), (2) and (3), crop yield depends on *LAI* and therefore, the latter is regarded as an integrative impact metric. From this, we propose that *LAI* measurements in crop plants subjected to ashfall offer a new method for analysing crop

480 vulnerability and assessing potential yield loss for ash mass loads below the threshold (~6-30 kg m^{-2}) of direct mechanical damage to plants. The rapidly increasing ability to monitor crop characteristics, including type, *LAI* and biomass, using optical and radar earth observation

483 data (Hosseini et al., 2015; Fang et al., 2019; Rosso et al., 2022) provides an unprecedented opportunity to collect a spatially- and time-resolved information that can support the development of more realistic and more complete ash-loss of crop production relationships.

486 In order to unlock the full potential of *LAI* estimates for investigating the vulnerability of crops to ash events, more knowledge on how ash coatings on leaves interfere with *LI* is required. In our model of potential yield loss in tomato and chilli pepper (Fig. 6), we equated

489 *LAI* reduction with the foliar cover percentage covered with ash. In essence, this means that an ash deposit on leaves renders light interception inoperative. This may not always be the case because *LI* by a crop canopy is determined not only by the *LAI* of the species, but also by

492 the light absorption characteristics of the leaves (Liang et al., 2012), here modified by the ash deposit. Further laboratory investigations can generate the empirical observations needed to better constrain the changes in *LI* in relation to the characteristics (thickness/mass load, grain

495 size, albedo) of the ash material deposited onto the leaf surface.

The evolution of *LAI* following an ash deposition event (Fig. 5a) was modelled by assuming that ash-affected plants will grow new leaves after a set period of time. Our analysis showed that *CYL*$_\%$ is sensitive to this parameter, therefore requiring adjustment depending on crop type (Klepper et al., 1982). We also note that many crops (including major ones such as wheat; Hay and Porter, 2006) have a determinate growth habit and as such, may not be able to sprout new leaves if they receive ash late in their development cycle. Another assumption made to evaluate the *LAI* trend over time is that the entire plant canopy received the same amount of ash. Although this was verified for tomato and chilli pepper when at the seven- and eight-leaf stage, respectively, it may not be necessarily the case at a later stage of their growth if upper leaves partly shield the surfaces of leaves located below them from direct exposure to ash. Thus, the effect of ashfall on crop *LAI* hinges both on plant growth characteristics and timing of the volcanic eruption. We considered in our model that an ash deposit induces premature leaf senescence, in agreement with field observations (Miller, 1967; Neild et al., 1998; Wilson et al., 2007; Ligot et al., 2022). While this process probably relates to leaf chlorosis due to *LI* reduction (Bilderback 1897; Mack, 1981; Ligot et al., 2022), its temporality and precise mechanism remain unclear. New experimental investigations with various crop plants will help to better constrain the proportion of leaf biomass affected by ash which will be subjected to premature senescence.

We have highlighted that grain size, leaf pubescence and humidity conditions at leaf surfaces control ash retention, which in turn drives *LAI* reduction. Other factors may influence ash retention. For example, leaf microstructural features such as stomatal density and presence of a waxy epicuticle have been shown to influence retention of non-volcanic dust particles (Sæbø et al., 2012; Zhang et al., 2017). In addition, in the natural environment, wind- and rain-driven erosion processes can remove ash deposited on foliage. Conversely, light rain may induce crusting of ash, prolonging its residence time on leaves (Miller, 1966; Ayris and

498

501

504

507

510

513

516

519

Delmelle, 2012; Le Pennec et al., 2012; Ligot et al., 2022). The significance of these

522 environmental variables in controlling ash retention time by leaves has never been assessed

quantitatively, calling for further field and experimental investigations linking ash residence

time on plants and impacts.

525 Finally, our approach for modelling production loss in tomato and chilli pepper exposed to

ash neglects impact to flowers or harvested plant parts, and assumes that light interception is

the main variable governing plant growth. While this is true in our study where water and

528 nutrient supply were never limited, more stringent conditions may be encountered in crop

fields subjected to ashfall. For example, an ash layer on the ground may alter water and gas

movements into and through the soil and surface runoff (Ayris and Delmelle, 2012; Neslon,

531 2013; Tarasenko, 2018), in turn impacting the soil water balance. A better comprehension of

the side effects of ash deposition on the soil plant-system is needed in order to identify the

primary mechanisms driving the short- and long-term consequences for crop production.

534 **Conclusions**

Our study highlights the usefulness of conducting experimental measurements to supplement

observations obtained from post-*EIA*. It provides a new perspective into the volcanic and non-

537 volcanic factors that control ash impact on crops. The experimental results obtained for

tomato and chilli pepper plants demonstrate that ash retention on leaf surfaces increases with

decreasing grain size and is enhanced when leaves are pubescent and wet. We also showed

540 that, for a given ash mass load (~570 g m^{-2}), the leaf surface percentage covered with ash is an

exponential decay function of grain size of which the parameters are influenced by leaf

pubescence and humidity conditions at leaf surfaces. Thus, we conclude that the proportion of

543 fine material in ash fallout is an important hazard metric for assessing risk to crops. The

corollary to this finding is that relying on ash thickness (or mass load) alone to anticipate crop damage from ash is inaccurate and possibly misleading.

546   Using the empirical relationship linking ash retention to ash grain size and equating ash retention with LAI reduction, we have developed a novel model framework to predict $CYL_\%$. This approach identifies LAI as a promising impact metric that can be quantified for assessing

549   crop production following an ashfall event. LAI is commonly retrieved *via* remote sensing measurements. The rapid deployment of new satellites allows data collection at increasingly high spatial and temporal resolution (for example, the European Space Agency's Sentinel-2

552   mission), paving the way for estimating LAI at the crop field scale. Additionally, the technology gives access to $FPAR$, i.e. the fraction of the solar radiation absorbed by live leaves for the photosynthesis activity, which should also record a reduction in light

555   interception for leaves covered with ash. We anticipate that tapping into satellite-derived measurements will considerably improve our quantitative understanding of crop vulnerability to ash fallout. However, for exploiting their full potential, field- and laboratory-based

558   validations are required, including experiments aimed at constraining LI/LAI reduction in relation to ash retention and characteristics. Acquiring this knowledge will significantly enhance our capacity to estimate ash-related risks to crops accurately. Governments and

561   payout agencies need such assessments in order to develop and implement effective risk reduction strategies for ashfall damage to crops in volcanically active agricultural regions.

Code availability

564   The Image J macro to analyse the plant photos and estimate the foliar cover coated with ash and the R script to compute the daily tomato and chilli pepper LAI, LI, $CBIO_c$ and $CYL_\%$ are available on GitHub (https://github.com/NoaLigot/ImageJ-macro.git and

567 https://github.com/NoaLigot/R-scipt-LAI-LI-biomass-yield-loss/blob/main/script,

respectively).

Data availability

570 All raw data can be provided by the corresponding author upon request.

Author contribution

NL, PD and GL conceptualized the experiments and NL carried them out. PB advised on the

573 statistical analysis and modelling approach. NL analysed the data, wrote the R script and ran

the simulations with the help of SB. NL and PD wrote the original draft with contributions

from all co-authors. PD secured funding for this research and provided the resources.

576 **Competing interests**

The authors declare that they have no conflict of interest.

Acknowledgements

579 N.L.'s doctoral research is supported by the FSR-FNRS (Fonds National de la Recherche

Scientifique 1.E077.19). N.L. is grateful to VOCATIO for a Fonds Ernest Solvay award that

contributed to support this study. This work was partly funded by a UCLouvain FSR-ARC,

582 "Talos" research grant (20/25-106). N.L. and P.D. are indebted to Marc Migon (SEFY, Earth

and Life Institute) for technical assistance, Xavier Draye (Earth and Life Institute) for lending

the camera equipment and Karen Fontijn (Department of Geosciences, Environment and

585 Society, Université Libre de Bruxelles) for access to ash sieving facility.

References

588   Al Mamun Hossain, S. A., Lixue, W., Chen, T., and Li, Z.: Leaf area index assessment for

tomato and cucumber growing period under different water treatments, Plant Soil Environ.,

63, doi: 10.17221/568/2017-PSE, 2017.

591   Arnalds, O.: The influence of volcanic tephra (ash) on ecosystems, in: Adv. Agron., edited by:

Sparks, D. L., Academic Press, 331-380, doi: 10.1016/B978-0-12-407685-3.00006-2, 2013.

Ayris, P. M. and Delmelle, P.: The immediate environmental effects of tephra emission, Bull.

594   Volcanol., 74, 1905-1936, doi: 10.1007/s00445-012-0654-5, 2012.

Bagheri, G. and Bonadonna, C.: Chapter 2 - Aerodynamics of volcanic particles:

characterization of size, shape, and settling velocity, in: Volcanic Ash, edited by: Mackie, S.,

597   Cashman, K., Ricketts, H., Rust, A., and Watson, M., Elsevier, 39-52, doi: 10.1016/B978-0-

08-100405-0.00005-7, 2016.

Benson, H., Benson, H. (Ed.): Physique I: Mécanique, 5th, De Boeck Supérieur, 2015.

600   Bhushan, B. and Jung, Y. C.: Micro- and nanoscale characterization of hydrophobic and

hydrophilic leaf surfaces, Nanotechnology, 17, 2758, doi: 10.1088/0957-4484/17/11/008,

2006.

603   Biass, S., Jenkins, S. F., Aeberhard, W. H., Delmelle, P., and Wilson, T.: Insights into the

vulnerability of vegetation to tephra fallouts from interpretable machine learning and big

Earth observation data, Nat. Hazards Earth Syst. Sci, 2022, 1-55, doi: 10.5194/nhess-2022-79,

606   2022.

Bilderback , D. E.: Mount St. Helens 1980: botanical consequences of the explosive

eruptions, University of California Press, 1897.

609   Biscoe, P. V., Gallagher, J. N., Landsberg, J. J., and Cutting, C. V.: Weather, dry matter

production and yield, in: Environmental Effects on Crop Physiology, Landsberg, J. J.&

Cutting, C. V. ed., AcademicPress, London, 75-100, 1977.

612   Blake, D. M., Hayes, J. L., Andreastuti, S., Hendrasto, M., Wilson, G., Jenkins, S. F.,

Daniswara, R., Cronin, S., Stewart, C., Wilson, T. M., Ferdiwijaya, D., Craig, H. M., Horwell,

C. J., and Leonard, G. S.: The 2014 eruption of Kelud volcano, Indonesia: impacts on

615   infrastructure, utilities, agriculture and health, New Zealand, 130 pp., 2015.

Blong, R.: The effects on agriculture, in: Volcanic Hazards: a sourcebook on the effects of

eruptions, Academic Press, London, 311-350, doi: 10.1016/0166-3097(86)90025-8, 1984.

618   Brown, S. K., Auker, M. R., and Sparks, R. S. J.: Populations around Holocene volcanoes and

development of a Population Exposure Index, in: Global Volcanic Hazards and Risk, edited

by: Vye-Brown, C., Brown, S. K., Sparks, S., Loughlin, S. C., and Jenkins, S. F., Cambridge

621   University Press, Cambridge, 223-232, doi: 10.1017/CBO9781316276273.006, 2015.

Burket, S. D., Furlow, E. P., Golding, P. R., Grant, L. C., Lipovsky, W. A., and Lopp, T. G.:

The economic effects of the eruptions of Mt. St. Helens, United States International Trade

624   Commission, Washington, D.C. 20438, 84 pp., 1980.

Campillo, C., García, M. I., Daza, C., and Prieto, M. H.: Study of a non-destructive method

for estimating the leaf area index in vegetable crops using digital images, HortScience, 45,

627   1459-1463, doi: 10.21273/hortsci.45.10.1459, 2010.

Chamberlain, A. C.: Transport of Lycopodium spores and other small particles to rough

surfaces, Proc. R. Soc. Lond. A, 296, 45-70, doi: 10.1098/rspa.1967.0005, 1967.

630   Chamberlain, A. C. and Chadwick, R. C.: Deposition of spores and other particles on

vegetation and soil, Ann. Appl. Biol., 71, 141-158, doi: 10.1111/j.1744-7348.1972.tb02949.x,

1972.

633   Coltelli, M., Miraglia, L., and Scollo, S.: Characterization of shape and terminal velocity of

tephra particles erupted during the 2002 eruption of Etna volcano, Italy, Bull. Volcanol., 70,

1103-1112, doi: 10.1007/s00445-007-0192-8, 2008.

636 Cook, R. J., Barron, J. C., Papendick, R. I., and Williams, G. J.: Impact on agriculture of the

mount St. Helens eruptions, Science, 211, 16-22, doi: 10.1126/science.211.4477.16, 1981.

Costa, A., Pioli, L., and Bonadonna, C.: Assessing tephra total grain-size distribution: insights

639 from field data analysis, Earth. Planet. Sci. Lett., 443, 90-107, doi:

10.1016/j.epsl.2016.02.040, 2016.

Craig, H., Wilson, T., Magill, C., Stewart, C., and Wild, A. J.: Agriculture and forestry impact

642 assessment for tephra fall hazard: fragility function development and New Zealand scenario

application, Volcanica, 4, 345 - 367, doi: 10.30909/vol.04.02.345367, 2021.

Craig, H., Wilson, T., Stewart, C., Outes, V., Villarosa, G., and Baxter, P.: Impacts to

645 agriculture and critical infrastructure in Argentina after ashfall from the 2011 eruption of the

Cordón Caulle volcanic complex: an assessment of published damage and function

thresholds, J. Appl. Volcanol., 5, 7, doi: 10.1186/s13617-016-0046-1, 2016a.

648 Craig, H., Wilson, T., Stewart, C., Villarosa, G., Outes, V., Cronin, S., and Jenkins, S.:

Agricultural impact assessment and management after three widespread tephra falls in

Patagonia, South America, Nat. Hazards, 82, 1167-1229, doi: 10.1007/s11069-016-2240-1,

651 2016b.

Craig, H. M.: Agricultural vulnerability to tephra fall impacts., Geology, University of

Canterbury, Canterbury, 375 pp., 2015.

654 Darge, A., Sharma R, D. R., Zerihum, D., and Chung, P. Y. K.: Multi color image

segmentation using L*A*B* color space, International Journal of Advanced Engineering,

Management and Science, 5, 346-352, doi: 10.22161/IJAEMS.5.5.8, 2019.

657 de Guzman, E. M. The Pinatubo eruption of June 1991: the nature and impact of the disaster.

(18 p.). Asian Disaster Reduction Center https://reliefweb.int/report/philippines/eruption-

mount-pinatubo-philippines-june-1991 (last access: 31 July 2022), 2005.

660   Dellino, P., Mele, D., Bonasia, R., Braia, G., La Volpe, L., and Sulpizio, R.: The analysis of

the influence of pumice shape on its terminal velocity, Geophys. Res. Lett., 32, 1-4, doi:

10.1029/2005gl023954, 2005.

663   Eggler, W. A.: Plant communities in the vicinity of the volcano El Paricutin, Mexico, after

two and a half years of eruption, Ecology, 29, 415-436, doi: 10.2307/1932635, 1948.

Elia, A. and Conversa, G.: Agronomic and physiological responses of a tomato crop to

666   nitrogen input, Eur. J. Agron., 40, 64-74, doi: 10.1016/j.eja.2012.02.001, 2012.

Eychenne, J., Le Pennec, J.-L., Troncoso, L., Gouhier, M., and Nedelec, J.-M.: Causes and

consequences of bimodal grain-size distribution of tephra fall deposited during the August

669   2006 Tungurahua eruption (Ecuador), Bull. Volcanol., 74, 187-205, doi: 10.1007/s00445-011-

0517-5, 2012.

Fang, H., Frederic, B., Plummer, S., and Schaepman-Strub, G.: An overview of global leaf

672   area Index (LAI): methods, products, validation, and applications, Rev. Geophys., 57, doi:

10.1029/2018RG000608, 2019.

FAO (Food and Agriculture Organisation): The impact of disasters and crises on agriculture

675   and food security: 2021, Rome, 245 pp., doi: 10.4060/cb3673en, 2021.

Farrokhi, E., Nassiri Mahallati, M., Koocheki, A., and Beheshti, S. A.: Light extinction

coefficient and radiation use efficiency in different growth stages of tomato exposed to

678   different irrigation regimes, Env. Stresses Crop Sci., 14, 629-648, doi:

10.22077/escs.2020.2960.1762, 2021.

Fierstein, J. and Nathenson, M.: Another look at the calculation of fallout tephra volumes,

681   Bull. Volcanol., 54, 156-167, doi: 10.1007/BF00278005, 1992.

Freire, S., Florczyk, A. J., Pesaresi, M., and Sliuzas, R.: An improved global analysis of

population distribution in proximity to active volcanoes, 1975-2015, ISPRS Int. J. Geoinf., 8,

684   341, doi: 10.3390/ijgi8080341, 2019.

Gallardo, M., Thompson, R. B., Giménez, C., Padilla, F. M., and Stöckle, C. O.: Prototype

decision support system based on the VegSyst simulation model to calculate crop N and water

687   requirements for tomato under plastic cover, Irrig. Sci., 32, 237-253, doi: 10.1007/s00271-

014-0427-3, 2014.

Gregory, P. H.: The microbiology of the atmosphere, 1st, L. Hill, London, doi:

690   10.5962/bhl.title.7291, 1961.

Grishin, S. Y., del Moral, R., Krestov, P. V., and Verkholat, V. P.: Succession following the

catastrophic eruption of Ksudach volcano (Kamchatka, 1907), Vegetatio, 127, 129-153, doi:

693   10.1007/BF00044637, 1996.

Hatfield, J.: Radiation use efficiency: evaluation of cropping and management systems,

Agron. J., 106, 1820, doi: 10.2134/agronj2013.0310, 2014.

696   Hay, R. K. M.: Harvest index: A review of its use in plant breeding and crop physiology,

Ann. Appl. Biol., 126, 197-216, doi: 10.1111/j.1744-7348.1995.tb05015.x, 2008.

Hay, R. K. M. and Porter, J. R.: The physiology of crop yield, 2nd, Blackwell Publishing, 314

699   pp., doi: 10.1017/S0014479707005595, 2006.

Higashide, T., Yasuba, K.-i., Suzuki, K., Nakano, A., and Ohmori, H.: Yield of japanese

tomato cultivars has been hampered by a breeding focus on flavor, HortScience, 47, 1408-

702   1411, doi: 10.21273/hortsci.47.10.1408, 2012.

Hirano, T., Kiyota, M., and Aiga, I.: The effects of dust by covering and plugging stomata and

by increasing leaf temperature on photosynthetic rate of plant leaves, J. Agric. Meteorol., 46,

705   215-222, doi: 10.2480/agrmet.46.215, 1991.

Hirano, T., Kiyota, M., and Aiga, I.: Physical effects of dust on leaf physiology of cucumber

and kidney bean plants, Environ. Pollut., 89, 255-261, doi: 10.1016/0269-7491(94)00075-O,

708   1995.

Hirano, T., Kiyota, M., Kitaya, Y., and Aiga, I.: The physical effects of dust on

photosynthetic rate of plant leaves, J. Agric. Meteorol., 46, 1-7, doi: 10.2480/agrmet.46.1,

711   1990.

Hirano, T., Kiyota, M., Seki, K., and Aiga, I.: Effects of volcanic ashes from Mt. Unzen-

Fugendake and Mt. Sakurajima on leaf temperature and stomatal conductance of cucumber, J.

714   Agric. Meteorol., 48, 139-145, doi: 10.2480/agrmet.48.139, 1992.

Hosseini, M., McNairn, H., Merzouki, A., and Pacheco, A.: Estimation of Leaf Area Index

(LAI) in corn and soybeans using multi-polarization C- and L-band radar data, Remote Sens.

717   Environ., 170, 77-89, doi: 10.1016/j.rse.2015.09.002, 2015.

Israelachvili, J. N., Burlington, U. (Ed.): Intermolecular and surface forces, 3rd, Academic

Press, Burlington, MA, 2011.

720   Jenkins, S. F., Spence, R. J. S., Fonseca, J. F. B. D., Solidum, R. U., and Wilson, T. M.:

Volcanic risk assessment: quantifying physical vulnerability in the built environment, J.

Volcanol. Geotherm. Res., 276, 105-120, doi: 10.1016/j.jvolgeores.2014.03.002, 2014.

723   Jenkins, S. F., Wilson, T. M., Magill, C. R., Miller, V., Stewart, C., W., M., and Boulton, M.:

Volcanic ash fall hazard and risk: technical background paper for the UNISDR Global

Assessment Report on Disaster Risk Reduction 2015, Global Volcano Model and IAVCEI, 43

726   pp., 2015.

Jenkins, S. F., Biass, S., Williams, G. T., Hayes, J. L., Tennant, E., Yang, Q., Burgos, V.,

Meredith, E. S., Lerner, G. A., Syarifuddin, M., and Verolino, A.: Evaluating and ranking

729   Southeast Asia's exposure to explosive volcanic hazards, Nat. Hazards Earth Syst. Sci, 22,

1233-1265, doi: 10.5194/nhess-22-1233-2022, 2022.

Jenkins, S. F., Biass, S., Williams, G. T., Hayes, J. L., Tennant, E. M., Yang, Q., Burgos, V.,

732   Meredith, E. S., Lerner, G. A., Syarifuddin, M., and Verolino, A.: Evaluating and ranking

Southeast Asia's exposure to explosive volcanic hazards, Nat. Hazards Earth Syst. Sci, 2021, 1-49, doi: 10.5194/nhess-2021-320. Preprint., 2021.

735   Johnson, J. E. and Lovaas, A. I.: Progress report on simulated fallout studies, Colorado State University, pp., 1969.

Karam, F., Masaad, R., Bachour, R., Rhayem, C., and Rouphael, Y.: Water and radiation use

738   efficiencies in drip-irrigated pepper (Capsicum annuum L.): response to full and deficit irrigation regimes, Eur. J. Hortic. Sci., 74, 79-85, 2009.

Kemanian, A. R., Stöckle, C. O., Huggins, D. R., and Viega, L. M.: A simple method to

741   estimate harvest index in grain crops, Field Crops Res., 103, 208-216, doi: 10.1016/j.fcr.2007.06.007, 2007.

Kleinhenz, V., Katroschan, K.-U., Schütt, F., and Stützel, H.: Biomass accumulation and

744   partitioning of tomato under protected cultivation in the humid tropics, Eur. J. Hort. Sci., 71, 173-182, 2006.

Klepper, B., Rickman, R. W., and Peterson, C. M.: Quantitative characterization of vegetative

747   development in small cereal grains, Agron. J., 74, 789-792, doi: 10.2134/agronj1982.00021962007400050005x, 1982.

Le Guern, F., Bernard, A., and Chevrier, R. M.: Soufrière of guadeloupe 1976–1977 eruption

750   — mass and energy transfer and volcanic health hazards, Bulletin Volcanologique, 43, 577-593, doi: 10.1007/BF02597694, 1980.

Le Pennec, J.-L., Ruiz, G. A., Ramón, P., Palacios, E., Mothes, P., and Yepes, H.: Impact of

753   tephra falls on Andean communities: the influences of eruption size and weather conditions during the 1999–2001 activity of Tungurahua volcano, Ecuador, J. Volcanol. Geotherm. Res., 217-218, 91-103, doi: 10.1016/j.jvolgeores.2011.06.011, 2012.

756   Liang, S., Li, X., and Jindi, W.: Advanced remote sensing : terrestrial information extraction and applications, 1st, Elsevier, 2012.

Ligot, N.: Crop vulnerability to tephra fall in volcanic regions: field, experimental and

759   modelling approaches, Earth and Life Institute, UCLouvain, Belgium, 285 pp., 2022.

Ligot, N., Guevara C, A., and Delmelle, P.: Drivers of crop impacts from tephra fallout:

insights from interviews with farming communities around Tungurahua volcano, Ecuador,

762   Volcanica, 5, 163-181, doi: 10.30909/vol.05.01.163181, 2022.

Mack, R. N.: Initial effects of ashfall from mount St. Helens on vegetation in eastern

Washington and adjacent Idaho, Science, 213, 537-539, doi: 10.1126/science.213.4507.537,

765   1981.

Magill, C., Wilson, T., and Okada, T.: Observations of tephra fall impacts from the 2011

Shinmoedake eruption, Japan, Earth Planets Space, 65, 18, doi: 10.5047/eps.2013.05.010,

768   2013.

Martínez-Ruiz, A., Lopez-Cruz, I., Ruiz Garcia, A., Pineda, J., and Prado hernández, J.:

HortSyst: a dynamic model to predict growth, nitrogen uptake, and transpiration of

771   greenhouse tomatoes, Chil. J. Agric. Res., 79, 89-102, doi: 10.4067/S0718-

58392019000100089, 2019.

McLaren, K.: XIII—The development of the CIE 1976 (L* a* b*) uniform colour space and

774   colour-difference formula, J. Soc. Dye. Colour., 92, 338-341, doi: 10.1111/j.1478-

4408.1976.tb03301.x, 1976.

Mendoza Perez, C., Ojeda, W., Carlos, R., and Flores, H.: Estimation of leaf area index and

777   yield of greenhouse-grown poblano pepper, Ing. agric. biosist., 9, 37-50, doi:

10.5154/r.inagbi.2017.04.009, 2017.

Miller, C. F.: The contamination behavior of fallout-like particles ejected by volcano Irazu,

780   Stanford Research Institute, San Francisco, California, MU-5779, 61 pp., 1966.

Miller, C. F.: Operation ceniza-arena: The retention of fallout particles from volcan Irazu (Costa Rica) by plant and people. Part 2, Stanford Research Institute, San Francisco,

783   California, MU-4890, 247 pp., 1967.

Monte, J. A., de Carvalho, D. F., Medici, L. O., da Silva, L. D. B., and Pimentel, C.: Growth analysis and yield of tomato crop under different irrigation depths, Rev. Bras. de Eng.

786   Agricola e Ambient., 17, 926 – 931, doi: 10.1590/S1415-43662013000900003, 2013.

Monteith, J. L.: Light Interception and radiative exchange in crop stands, in: Physiological Aspects of Crop Yield, edited by: Easton Jerry D. , Haskins F.A. , Sullivan C.Y. , and van

789   Bavel C.H.M., American Society of Agronomy, Wisconsin, 89-115, doi: 10.2135/1969.physiologicalaspects.c9, 1969.

Monteith, J. L.: Solar radiation and productivity in tropical ecosystems, J. Appl. Ecol., 9, 747-

792   766, doi: 10.2307/2401901, 1972.

Monteith, J. L.: Climate and the efficiency of crop production in Britain Philosophical Transactions of the Royal Society of London. Series B, Biological Sciences, 281, 277-294,

795   1977.

Neild, J., O'Flaherty, P., Hedley, P., Underwood, R., Johnston, D., Christenson, B., and Brown, P.: Impact of a volcanic eruption on agriculture and forestry in New Zealand,

798   Ministry of Agriculture and Forestry, New Zealand, 99/2, 88 pp., 1998.

Neslon, G. L. M.: Land rehabilitation techniques of rice farmers in Pampanga (Philippines) after the Mt. Pinatubo eruption, Asia Life Sci., 22, 155-181, 2013.

801   Newhall, C. G. and Self, S.: The volcanic explosivity index (VEI): an estimate of explosive magnitude for historical volcanism, J. Geophys. Res., 87, 1231-1238, doi: 10.1029/JC087iC02p01231, 1982.

804   Niklas, K. J.: A mechanical perspective on foliage leaf form and function, New Phytol., 143, 19-31, doi: 10.1046/j.1469-8137.1999.00441.x, 1999.

Nurfiani, D. and Bouvet de Maisonneuve, C.: Furthering the investigation of eruption styles

807   through quantitative shape analyses of volcanic ash particles, J. Volcanol. Geotherm. Res.,

354, doi: 10.1016/j.jvolgeores.2017.12.001, 2017.

Onofri, A. The broken bridge between biologists and statisticians: A blog and R package.

810   https://github.com/OnofriAndreaPG/aomisc (last access: 02 February 2022), 2020.

Pinheiro, J. and Bates, D. Package 'nlme'. (338 p.). The Comprehensive R Archive Network

https://cran.r-project.org/web/packages/nlme/nlme.pdf (last access: 31 July 2022), 2022.

813   Poorter, H., Jagodziński, A., Ruiz-Peinado, R., Kuyah, S., Luo, Y., Oleksyn, J., Usol'tsev, V.,

Buckley, T., Reich, P., and Sack, L.: How does biomass distribution change with size and

differ among species? An analysis for 1200 plant species from five continents, New Phytol.,

816   208, doi: 10.1111/nph.13571, 2015.

Ram, S. S., Majumder, S., Chaudhuri, P., Chanda, S., Santra, S. C., Maiti, P. K., Sudarshan,

M., and Chakraborty, A.: Plant canopies: bio-monitor and trap for re-suspended dust

819   particulates contaminated with heavy metals, Mitig. Adapt. Strateg. Glob. Chang., 19, 499-

508, doi: 10.1007/s11027-012-9445-8, 2012.

Rosso, P., Nendel, C., Gilardi, N., Udroiu, C., and Chlébowski, F.: Processing of remote

822   sensing information to retrieve leaf area index in barley: a comparison of methods, Precis.

Agric., doi: 10.1007/s11119-022-09893-4, 2022.

Rust, A. and Cashman, K.: Permeability controls on expansion and size distributions of

825   pyroclasts, J. Geophys. Res. Solid Earth, 116, 1-17, doi: 10.1029/2011JB008494, 2011.

Sæbø, A., Popek, R., Nawrot, B., Hanslin, H. M., Gawronska, H., and Gawronski, S. W.:

Plant species differences in particulate matter accumulation on leaf surfaces, Sci. Total

828   Environ., 427-428, 347-354, doi: 10.1016/j.scitotenv.2012.03.084, 2012.

Schindelin, J., Rueden, C. T., Hiner, M. C., and Eliceiri, K. W.: The ImageJ ecosystem: an open platform for biomedical image analysis, Mol. Reprod. Dev., 82, 518-529, doi:

831 10.1002/mrd.22489, 2015.

Small, C. and Naumann, T.: The global distribution of human population and recent volcanism, Environ. Hazards, 3, 93-109, doi: 10.3763/ehaz.2001.0309, 2001.

834 Smith, W. H. and Staskawicz, B. J.: Removal of atmospheric particles by leaves and twigs of urban trees: some preliminary observations and assessment of research needs, Environ. Manage., 1, 317-330, doi: 10.1007/BF01865859, 1977.

837 Solargis. Solar resource maps of Belgium. https://solargis.com/maps-and-gis-data/download/belgium (last access: 17 March 2022), 2022.

Starr, J. R.: Inertial impaction of particulates upon bodies of simple geometry, Ann. Occup.

840 Hyg., 10, 349-361, doi: 10.1093/annhyg/10.4.349, 1967.

Surmaini, E., Hidayati, R., and Triwidiatno: Extinction coefficient and production of bushy pepper at several radiation levels, Indonesian Soil and Climate Journal, 18, doi:

843 10.2017/jti.v0n18.2000.%p, 2000.

Sword-Daniels, V., Wardman, J., Stewart, C., Wilson, T., Johnston, D., and Rossetto, T.: Infrastructure impacts, management and adaptations to eruptions at Volcán Tungurahua,

846 Ecuador, 1999-2010, Institute of Geological and Nuclear Sciences, New-Zealand, 90 pp., 2011.

Ta, H., Shin, J. H., Ahn, T. I., and Son, J. E.: Modeling of transpiration of paprika (Capsicum

849 annuum L.) plants based on radiation and leaf area index in soilless culture, Hortic. Environ. Biotechnol., 52, 265-269, doi: 10.1007/s13580-011-0216-3, 2011.

Tabor, D.: Surface forces and surface interactions, J. Colloid Interface Sci., 58, 3-14, doi:

852 10.1016/B978-0-12-404501-9.50009-2, 1977.

Tampubolon, J., Nainggolan, H. L., Ginting, A., and Aritonang, J.: Mount Sinabung eruption: Impact on local economy and smallholder farming in KaroRegency, North Sumatra, IOP

855   Conference Series: Earth and Environmental Science, 178, 012039, doi: 10.1088/1755-1315/178/1/012039, 2018.

Tarasenko, I.: Environmental effects of volcanic eruptions : A multidisciplinary study of

858   tephra impacts on plant and soil, Université catholique de Louvain, Belgium, 2018.

Thompson, J. R., Mueller, P. W., Flückiger, W., and Rutter, A. J.: The effect of dust on photosynthesis and its significance for roadside plants, Environ. Pollut. Control, 34, 171-190,

861   doi: 10.1016/0143-1471(84)90056-4, 1984.

UNDRO (Office of the United Nations Disaster Relief co-Ordinator): Natural disasters and vulnerability analysis: report of expert group meeting, 9-12 July 1979, UN, Geneva, 48 pp.,

864   1980.

Van den Bogaard, P. and Schmincke, H. U.: The eruptive center of the late quaternary Laacher See tephra, Geol. Rundsch., 73, 933-980, doi: 10.1007/BF01820883, 1984.

867   Vogel, S.: Drag and reconfiguration of broad leaves in high winds, J. Exp. Bot., 40, 941-948, doi: 10.1093/jxb/40.8.941, 1989.

Weraduwage, S. M., Chen, J., Anozie, F. C., Morales, A., Weise, S. E., and Sharkey, T. D.:

870   The relationship between leaf area growth and biomass accumulation in Arabidopsis thaliana, Front. Plant Sci., 6, doi: 10.3389/fpls.2015.00167, 2015.

Wilson, J. W.: Ecological data on dry-matter production by plants and plant communities, in:

873   The Collection and Processing of Field Data, edited by: Bradley, E. F., and Denmead, O. T., Interscience Publishers, New York, 1967.

Wilson, T. M. and Kaye, G. D.: Agricultural fragility estimates for volcanic ash fall hazards,

876   Institute of Geological and Nuclear Sciences, New-Zealand 51 pp., 2007.

Wilson, T. M., Kaye, G., Stewart, C., and Cole, J.: Impacts of the 2006 eruption of Merapi volcano, Indonesia, on agriculture and infrastructure, Institute of Geological and Nuclear

879 Sciences, New Zealand, 64 pp., 2007.

Wilson, T. M., Cole, J., Cronin, S., Stewart, C., and Johnston, D.: Impacts on agriculture following the 1991 eruption of Vulcan Hudson, Patagonia: lessons for recovery, Nat. Hazards,

882 57, 185-212, doi: 10.1007/s11069-010-9604-8, 2011.

Witherspoon, J. P. and Taylor, F. G., Jr.: Interception and retention of a simulated fallout by agricultural plants, Health Phys., 19, 493-499, doi: 10.1097/00004032-197010000-00003,

885 1970.

Wohletz, K. H.: Mechanisms of hydrovolcanic pyroclast formation: grain-size, scanning electron microscopy, and experimental studies, J. Volcanol. Geotherm. Res., 17, 31-63, doi:

888 doi.org/10.1016/0377-0273(83)90061-6, 1983.

Yildirim, M., Demirel, K., and Bahar, E.: Radiation use efficiency and yield of pepper (Capsicum annuum L. cv. California Wonder) under different irrigation treatments, J. Agric.

891 Sci. Technol, 19, 693-705, 2017.

Zhang, W., Wang, B., and Niu, X.: Relationship between leaf surface characteristics and particle capturing capacities of different tree species in Beijing, Forests, 8, 92, doi:

894 10.3390/f8030092, 2017.